

TWO-DIMENSIONAL BEAM-BEAM INVARIANT WITH APPLICATIONS TO HL-LHC

D. Kaltchev, TRIUMF, Vancouver, B.C., Canada

Abstract

Long-range beam-beam interactions represent the most severe limitation on the performance and achievable luminosity of a circular collider. The paper presents a two-dimensional nonlinear Courant-Snyder Invariant derived to first order in the beam-beam perturbation and based on the two-dimensional coefficients in the Fourier expansion of the Beam-beam Hamiltonian. Its validity in case of HL-LHC lattices with realistic beam-beam setup is verified with MadX tracking.

INTRODUCTION

Within the weak-strong model with neglected bunch-length effects, the total effect on the transverse motion of the weak-beam (or test) particle of the many long-range beam-beam (1r) collisions that it encounters with the strong-beam bunch is usually studied by tracking, either for $\sim 10^3$ turns (geometric distortions of the ellipse and footprint), or for a very long term (dynamic aperture). For the 1r occurring within the two main Interaction Regions of the LHC: IR5 and IR1, geometric aberrations can also be studied with Lie-algebraic methods. Previously, the case of **1D motion** (in the plane of collision) was treated – [1–3], based on, and gradually developing, the original single-head-on formalism of A. Dragt, [4,5] and A. Chao, [6]. By computing the effective Hamiltonian $h(J_x, \phi_x)$, the surfaces of constant h -value in action-angle J_x, ϕ_x space were found to agree well with tracking: far from resonances, the turn-by-turn test-particle actions lay on the curve $W_x = h/\mu_x = \text{const}$ (more simply, one can compare the r.m.s. distortion of the surfaces, aka smear).

We present a formula for the geometric distortion of the **two-dimensional** nonlinear (Courant Snyder) invariant valid to lowest order of the beam-beam parameter λ . The n -th collision ($n = 1, \dots, N_{1r}$), is described by the coefficients $C_{mk}(a_x, a_y; \theta_{\text{str}}^{(n)})$ in the Fourier-expansion of the long-range beam-beam Hamiltonian, written in terms of action-angle coordinates $\vec{J}, \vec{\phi}$ of the unperturbed motion: $H(\vec{a}, \vec{\phi}; \theta_{\text{str}}^{(n)})$. Here m, k are integers, N_{1r} is the total number of 1r around the ring, $\vec{a} = (a_x, a_y)$, where $a_{x,y} \equiv \sqrt{2J_{x,y}/\epsilon}$, are the test particle normalized amplitudes, ϵ is the emittance and $\theta_{\text{str}}^{(n)}$ are the strong-beam lattice parameters at the (longitudinal) location of the beam-beam collision.

The two-dimensional C_{mk} are very interesting by themselves, since they participate in resonance driving terms which may account for the long-term behaviour. In previous papers [7, 8], expressions for C_{mk} were presented valid at large amplitudes and large ~ 12 normalized separations, as required by the nominal beam-beam layout and a round collision optics in the HL-LHC [9], see also [10]. It was further

shown in [7] that the amplitude detuning, or beam-beam footprint, derivatives of C_{00} , agree well with tracking. Our goal is to further verify that invariant and C_{mk} are correct, focusing on 1r collisions (k and m cannot be both zero).

2D NONLINEAR INVARIANT FOR BEAM-BEAM

This section outlines the procedure that builds the CS-invariants $W_{x,y}$ using an effective Hamiltonian h .

The one-turn motion of the test particle with 4D coordinates $X = (x, p_x, y, p_y)$ is described by a symplectic map as follows: $X_{1\text{turn}} = M X_{\text{ini}}$,

$$M = \prod_{n=1}^{N_{1r}} M_n e^{if^{(n)}}; M_{N_{1r}+1}. \quad (1)$$

The map product $M_n e^{if^{(n)}}$: of a linear map and a Lie exponent describes motion from one 1r to the next. The factors: $f^{(n)}$, assumed to act on the same (initial) variable, are

$$f^{(n)}(x, y) = -H^{(n)}(x, y; \theta_{\text{str}}^{(n)}), \quad (2)$$

where H is in units of $\lambda \equiv \frac{N_b r_0}{\gamma}$, γ is the relativistic factor and N_b is the bunch population. For a general (head-on or 1r) collision, the coefficients are ([7, 8]):

$$\begin{aligned} C_{mk}(\vec{a}; \theta_{\text{str}}) &= \frac{1}{4\pi^2} \iint_0^{2\pi} H(\vec{a}; \theta_{\text{str}}) e^{-im\phi_x - ik\phi_y} d\phi_x d\phi_y \\ &= i^{m+k} \int_0^1 \frac{dt}{t g_r(t)} (\delta_m \delta_k - Q_m^x(t) Q_k^y(t)) \end{aligned} \quad (3)$$

$$Q_m^z(t) = \frac{i^{-m}}{2\pi} \int_0^{2\pi} e^{-im\phi_z - tP_z} d\phi_z;$$

$$P_z = \frac{1}{2} (\vec{a}_z \sin \phi_z + \vec{d}_z)^2, \quad z = (x, y)$$

$$\vec{a}_x = r a_x, \quad \vec{d}_x = d_x, \quad \vec{a}_y = \frac{a_y}{g_r(t)}, \quad \vec{d}_y = \frac{r d_y}{g_r(t)},$$

$$g_r(t) \equiv \sqrt{1 + (r^2 - 1)t}.$$

δ_m is the Krönecker delta function. In this paper $\delta_m \delta_k = 0$.

In Eq. (2), H depends on x, y and the parameter array $\theta_{\text{str}} = (D_{x,y}, \sigma_{x,y})$ – the real-space full separations $D_{x,y}$ and r.m.s. sizes $\sigma_{x,y}$ (omitting “strong” in σ). With the transform $\bar{x} = \sqrt{2J_x} \sin \phi_x$, $\bar{p}_x = \sqrt{2J_x} \cos \phi_x$ (and similar for y), H in Eq. (3) has been rewritten in terms of $a_{x,y}$. An exact anti-symmetry of IR is assumed, leading to $\theta_{\text{str}} \equiv (d_{x,y}, r)$, where $d_{x,y} = D_{x,y}/\sigma_{x,y}$ are normalized offsets (relative separations between the orbits of the colliding bunches) and $r \equiv \frac{\sigma_y}{\sigma_x}$ is the strong-beam sigma aspect ratio. Either $d_x \neq 0$ (in IR5), or $d_y \neq 0$ (in IR1) and also in general $r \neq 1$.

Symmetries in the Coefficients

One need calculate C_{mk} only for positive m and k and then use the fact that H is real. For fixed a_x, a_y and θ_{str} , negating an index follows the rules

$$\begin{aligned} C_{-m-k} &= (-1)^{m+k} C_{mk} \\ C_{-m k} &= (-1)^m C_{mk} \\ C_{m -k} &= (-1)^k C_{mk}. \end{aligned}$$

Further, the $1r$ occur at longitudinal locations spaced half bunch distance apart, positioned symmetrically on both sides of the interaction points IP5 and IP1. The symmetry implies that θ_{str} changes in a specific way from left (L) to right (R) side within the IR (anti-symmetry in optics), and from IR5 to IR1 (x and y planes switched). To take this into account, with “slot” (#) being the $1r$ number counted from from the IP, one first computes the four C_{mk} corresponding to a fixed slot, and then loops over the $N_{1r}/4$ slots. It can be shown that within a slot the following relations hold:

$$\begin{aligned} C_{km}(a_x, a_y; \theta_{\text{str}}^{1R}) &= C_{mk}(a_y, a_x; \theta_{\text{str}}^{5L}) \\ C_{km}(a_x, a_y; \theta_{\text{str}}^{1L}) &= C_{mk}(a_y, a_x; \theta_{\text{str}}^{5R}). \end{aligned} \quad (4)$$

Thus one can calculate C_{mk} for the $1r$ in IR5 and use Eq. (4) to find the coefficients for IR1. However, for this IR5 needs to be treated twice (the second time with the exchange $a_x \leftrightarrow a_y$). For fixed amplitudes, deducing the full set of coefficients that describes one of the insertions from the other is (unfortunately) found to be impossible.

Closed-Orbit and Gradient Perturbation

Denote with hats matrices corresponding to linear operators. The linear maps M_n , as well as the accumulated maps (to the n -th collision): $\bar{M}_n = M_1 M_2 \dots M_n$ are extracted from an optics code (MadX, [11]): assumed uncoupled, they are in a familiar manner given by $\beta_{x,y}^{(n)}, \alpha_{x,y}^{(n)}, \mu_{x,y}^{(n)}$ – the linear twiss parameters and betatronic phase advances at the $1r$. With $\beta_{x,y}, \alpha_{x,y}$ being their values for $n = N_{1r} + 1$ (matched Twiss parameters for the ring) the total phase advances $\bar{\mu} = (\mu_x, \mu_y)$ are found from the trace of the ring matrix $\bar{M} \equiv \bar{M}_{N_{1r}+1}$.

The coefficients Eq. (3) need to be corrected (see [12]), since the above matrices are 1 - computed w.r.t. the perturbed closed orbit and 2 - correspond to perturbed Twiss parameters for the ring. For the closed orbit, by Fourier-expanding the x, y -terms in H , one needs to replace: $C_{mk} \rightarrow C_{mk} - \Delta_{mk}^1$, where $\Delta_{mk}^1 = -i m \delta_{|m|-1} \delta_k \frac{r a_x}{d_x} (1 - e^{-d_x^2/2})$. Similarly, expanding H to second order in x, y gives $C_{mk} \rightarrow C_{mk} - \Delta_{mk}^2$, where

$$\begin{aligned} \Delta_{mk}^2 &= -\delta_{|k|} (\delta_{|m|-2} - 2\delta_m) \times \\ &\times r^2 a_x^2 e^{-\frac{1}{2}d_x^2} (1 - e^{-\frac{1}{2}d_x^2} + d_x^2) / (4d_x^2) - \\ &- \delta_m \delta_{|k|-2} a_y^2 (1 - e^{-\frac{1}{2}d_x^2}) / (4d_x^2) \end{aligned}$$

with δ assuring that only $C_{\pm 1, \pm 1}, C_{\pm 2, \pm 2}$ are affected. The new coefficients $C_{mk} - \Delta_{mk}^1 - \Delta_{mk}^2$ are substituted in h .

It has been shown [12] that the effective Hamiltonian h is a straight-forward generalization of the 1D case:

$$\begin{aligned} h(\vec{J}, \vec{\phi}, \vec{\mu}) &= -\mu_x J_x - \mu_y J_y + S(\vec{J}, \vec{\phi}, \vec{\mu}); \quad (5) \\ S(\vec{J}, \vec{\phi}, \vec{\mu}) &\equiv \lambda \sum_{n=1}^{N_{1r}} \sum_{mk=-N_c}^{N_c} C_{mk}(a_x, a_y; \theta_{\text{str}}^{(n)}) \times \\ &\frac{(m\mu_x + k\mu_y)}{2 \sin \frac{1}{2}(m\mu_x + k\mu_y)} e^{im(\frac{\mu_x}{2} + \phi_x + \mu_x^{(n)}) + ik(\frac{\mu_y}{2} + \phi_y + \mu_y^{(n)})}. \end{aligned}$$

The derivation of Eq. (5) follows [13].

The S above is expanded as follows: $S(\vec{J}, \vec{\phi}, \vec{\mu}) = \mu_x S_x(\vec{J}, \vec{\phi}) + \mu_y S_y(\vec{J}, \vec{\phi}) + \dots$. By neglecting all (...) -terms, the two invariants are $-h/\mu_z$, where $z = (x, y)$, see [6]:

$$\begin{aligned} W_x(J_x, \phi_x) &\equiv J_x - S_x(J_x, J_y^0, \phi_x, \frac{\pi}{2}), \\ W_y(J_y, \phi_y) &\equiv J_y - S_y(J_x^0, J_y, \frac{\pi}{2}, \phi_y). \end{aligned}$$

Finally, the desired curves $J_z(\phi_z)$, are implicitly given by

$$W_x(J_x, \phi_x) = W_x(J_x^0, \frac{\pi}{2}), \quad W_y(J_x, \phi_x) = W_y(J_y^0, \frac{\pi}{2}), \quad (6)$$

where for given $a_{x,y}$ the initial actions are $J_{x,y}^0 = \epsilon a_{x,y}^2$ and $\epsilon = 3.35 \cdot 10^{-10}$ m.rad ($\pi/2$ appears because of the \sin chosen in Eq. (3)). In the next section, the two solutions of Eq. (6) are plotted over the interval $-\pi < \phi_{x,y} < \pi$.

RESULTS

A first-order BCH formula is used to derive h , hence it is clear that Eq. (5) also describes the lowest order distortions due to lattice multipoles (by redefining the strength λ). Such a test is performed on Fig. 1.

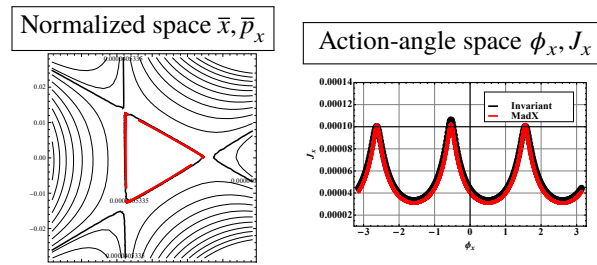


Figure 1: Contours of constant value of W_x , for a FODO cell containing several thin sextupoles tuned near third order resonance $(\mu_x, \mu_y)/(2\pi) = (0.335, 0.29)$ (left), and comparisons with MadX tracking (right).

Assuming (hypothetically) the $1r$ beam-beam to be the only nonlinearity present in the HL-LHC ring with nominal $1r$ setup – 18 $1r$ per IR side, spanning normalized separations 8 – 14 σ and $N_b = 1.1 \cdot 10^{11}$, the ability of $W_{x,y}$ to reproduce ring tracking at amplitudes approaching the strong-beam core is verified on Figs. 2 and 3. Here only

6 Fourier coefficients are used. In fact, as expected, the shape of the distorted invariant is dominated by terms up to and including octupole. For Fig. 2, the particle is launched in-plane (either $y = 0$ or $x = 0$) with increasing amplitude. Some disagreement is observed either for amplitudes too far from the strong-beam core (loss of numerical accuracy in case of vanishing smears, $< 1\%$) or, as it should be, when the particle penetrates the strong beam. Figure 3 shows off-plane tracking at “45-degree” initial angle, $a_x = a_y$. Since coupling is neglected, only the maximum excursions of the two curves approximately agree.

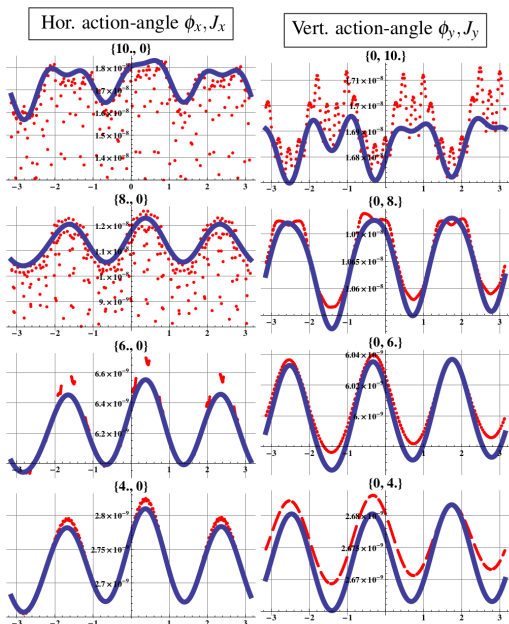


Figure 2: In-plane tracking around the ring ($N_{1r} = 4 \times 18$) of the weak-beam particle using MadX (red dots) and the projected invariants computed with 6 coefficients $N_c = 6$, Eq. (6) (blue). The particle is launched in either X (left) or Y (right) planes with $a_{x(y)} = 4, 6, 8$ and 10 . It penetrates the strong beam core at $\sim 8 \sigma$.

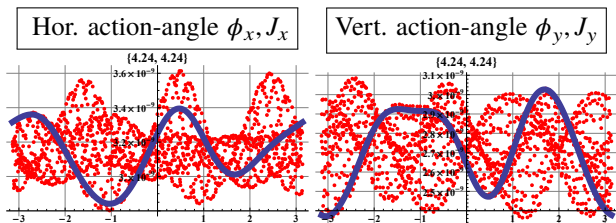


Figure 3: Off-plane tracking around the ring ($N_{1r} = 4 \times 18$): MadX (red) and projected invariants (blue). The particle is launched at combined amplitude = $6 (\times 1/\sqrt{2})$ on plots). Here again $N_c = 6$. The smear is $\sim 5\%$.

Another test concerns application of Hamiltonian driving-terms (HDT), see Introduction, in 1D, i.e. in the plane of collision, to the optimization of HL-LHC wire correctors – see [14] and references therein. Let, for some n in

Eq. (2), the $1r$ kicks correspond to wires (w) described by $H^{w(n)}$ and $C_{mk}^{w(n)}$. The total HDT, left or right of the IP, is $\sum_{L(R)} D_m^{l.r.} + D_m^{w(L,R)}$, where $D_m \equiv i^{-m} C_{m0}$ is real-valued. Notice that, compared with the two-dimensional resonance driving term (RDT) treatment in [14], the HDT defined here is in-plane (a disadvantage), but it depends on $a_{x,y}$ (advantage).

The following property has been demonstrated: there exists a *left-right independent* solution for the wires such that each of the above L and R sums can be reduced to zero simultaneously for all m and moreover, the solution is valid at all amplitudes outside (below) the strong beam core. Such a solution is tested on Figs. 4 and 5. Differently from [14], it corresponds to unequal parameters (distance to the axis and integrated current) for the left and right wire (they become equal only if the wire is installed at a location where $r = 1$).

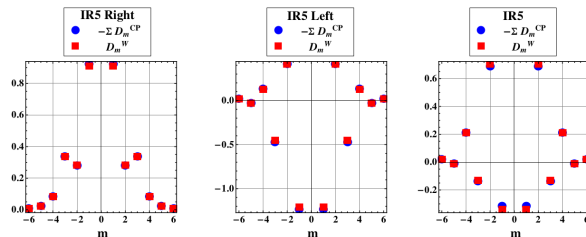


Figure 4: Simultaneous (for all m) cancellation of Hamiltonian driving terms in IR5 in case of the in-plane left-right independent wire correction explained in the text. The sum over the 18 $1r$ collision points $\sum D_m^{l.r.CP}$ (blue) is equal to $-D_m^w$ of the wire (red), both computed for $a_x = 6$. Similar plots result at lower amplitudes.

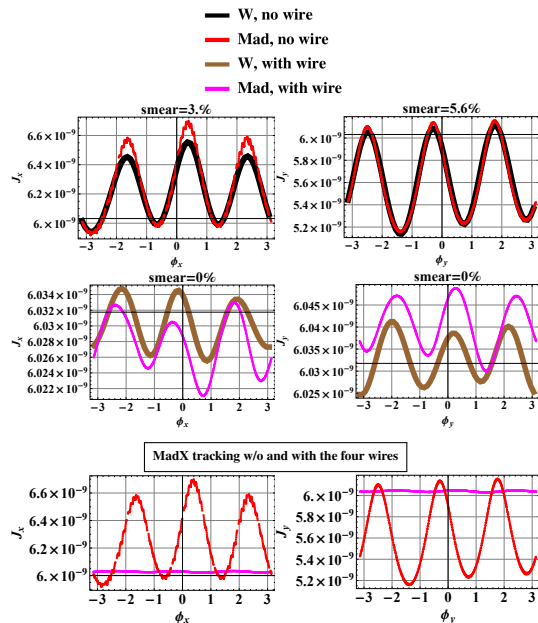


Figure 5: A test of the in-plane left-right independent wire correction. Two wires in IR5 are installed according to Fig. 4 and another two, symmetrically, in IR1. Tracking around the ring (MadX) with $(a_x, a_y) = (6, 0)$ (left plots) and $(a_x, a_y) = (0, 6)$ (right plots) and invariants $W_{x,y}$.

REFERENCES

- [1] D. Kaltchev, “On beam-beam resonances observed in LHC tracking”, TRIUMF, Vancouver, Canada, Rep. TRI-DN-07-9, March, 2007.
- [2] D. Kaltchev and W. Herr, “Analytical Calculation of the Smear for Long-Range Beam-Beam Interactions”, in *Proc. 23rd Particle Accelerator Conf. (PAC’09)*, Vancouver, Canada, May 2009, paper TH6PFP096, pp. 3934–3936.
- [3] D. Kaltchev and W. Herr, “Analysis of long range studies in the LHC - comparison with the model”, CERN, Geneva, Switzerland, Rep. CERN-2014-004.93, Mar. 2013.
- [4] A. J. Dragt and O. G. Jakubowicz, “Analysis of the Beam-Beam Interaction Using Transfer maps”, in *Proc. the Beam Beam Interaction Seminar*, Stanford, CA, May 22-23, 1980.
- [5] A. J. Dragt, “Transfer Map approach to the Beam-Beam interaction”, *AIP Conference Proceedings*, vol. 57, p. 143, 1980. doi:10.1063/1.32106
- [6] A. Chao, *Lie Algebra Techniques for Nonlinear Dynamics*, <http://www.slac.stanford.edu/>
- [7] D. Kaltchev, “Fourier Coefficients of Long-Range Beam-Beam Hamiltonian via Two-Dimensional Bessel functions”, in *Proc. 9th Int. Particle Accelerator Conf. (IPAC’18)*, Vancouver, Canada, Apr.-May 2018, pp. 3486–3488. doi:10.18429/JACoW-IPAC2018-THPAK108
- [8] D. Kaltchev, “Fourier expansion of Long Range Beam-Beam Hamiltonian”, TRIUMF, Vancouver, Canada, Rep. TRI-BN-1805, Apr. 2018.
- [9] Optics and layout repository for the third version of sLHC, <http://proj-lhc-optics-web.web.cern.ch/proj-lhc-optics-web/OpticsSourceAllVersions.link/SLHCV3.0/>
- [10] T. Sen *et al.*, “Beam-beam effects at the Fermilab Tevatron: Theory”, *Phys. Rev. ST Accel. Beams*, vol. 7, p. 041001, 2004. doi:10.1103/PhysRevSTAB.7.041001
- [11] MAD-X user’s guide, mad.web.cern.ch/mad
- [12] D. Kaltchev, “Derivation of a two-dimensional Beam-Beam invariant and applications to HL-LHC”, [arXiv.org](https://arxiv.org), in preparation.
- [13] J. Bengtsson and J. Irwin, “Analytical Calculation of Smear and Tune Shift”, CERN, Geneva, Switzerland, Rep. SSC-232, Feb. 1990.
- [14] S. Fartoukh, A. Valishev, Y. Papaphilippou, and D. Shatilov, “Compensation of the long-range beam-beam interactions as a path towards new configurations for the high luminosity LHC”, *Phys. Rev. ST Accel. Beams*, vol. 18, p. 121001, 2015. doi:10.1103/PhysRevSTAB.18.121001